Altered organization of light-harvesting complexes in phospholipid-enriched *Rhodobacter sphaeroides* chromatophores as determined by fluorescence yield and singlet-singlet annihilation measurements

Willem H.J. Westerhuis [1,a], Marcel Vos [b], Rienk van Grondelle [c], Jan Amesz [b], Robert A. Niederman [a,*]

[a] *Department of Molecular Biology and Biochemistry, Rutgers University, P.O. Box 1059, Piscataway, NJ 08855-1059, USA*
[b] *Department of Biophysics, Huygens Laboratory, State University, P.O. Box 9504, 2300 RA Leiden, The Netherlands*
[c] *Department of Biophysics, Physics Laboratory, Free University, De Boelelaan 1081, 1081 HV Amsterdam, The Netherlands*

Abstract

An improved method for fusion of liposomes to intracytoplasmic membrane vesicles of *Rhodobacter sphaeroides* was developed that involves repeated cycles of freeze-thaw-sonication and provides a controlled procedure for phospholipid enrichment of up to 15-fold. In freeze-fracture replicas, the fusion products appeared as closed vesicles of increased size and reduced intramembrane particle densities. Fluorescence yield measurements at 300 and 4 K showed that the gradual bilayer dilution was accompanied by reductions in energy transfer between the peripheral LH2 and core LH1 antennae, as well as from LH1 to reaction centers. Singlet-singlet annihilation at 4 K revealed a two-fold decrease in the cluster size of core antenna BChls, which was also reflected by changes in fluorescence polarization spectra. Energy transfer dynamics and structural considerations suggested that the annihilation curves were affected by non-uniformities. When taken into account, this led to the conclusion that in native membranes, on average two LH1-reaction center complexes are associated, that most peripheral antenna complexes are adjacent to at least one core assembly, and that fusion induces a separation of single LH1 and LH2 rings. At 4 K, a relatively large Stokes shift severely limits transfer between LH2 complexes in the native bilayer, while restricted transfer among two or three LH1 complexes arises mainly from spectral inhomogeneity. This explanation also implies that the anisotropic long-wavelength component of the LH1 absorption spectrum, which acts as an energy trap at 4 K, exists as an excitonic state involving 6–8 BChls. © 1998 Published by Elsevier Science B.V. All rights reserved.

Keywords: Light-harvesting complex; Photosynthesis; Energy transfer; Fluorescence spectroscopy; Singlet-singlet annihilation; Membrane fusion; (*Rhodobacter sphaeroides*)

---

* Corresponding author. Fax: +1 (732) 445-4213; E-mail: rniederm@rci.rutgers.edu
[1] Present address: Department of Molecular Biology and Biotechnology, University of Sheffield, Sheffield S10 2TN, UK.

1. Introduction

The photosynthetic units of the purple nonsulfur bacterium *Rhodobacter sphaeroides* are localized within the intracytoplasmic membrane (ICM) and contain three integral BChl-protein complexes: an LH2-type peripheral antenna (B800–850); an LH1-type core antenna (B875); and photochemical reaction centers. Both light-harvesting apoproteins consist of heterodimers of ∼5.5–7.0 kDa α- and β-polypeptides [1,2] that share a conserved tripartite structure [3], with a transmembrane α-helix separating N- and C-terminal domains at the cytoplasmic and periplasmic surfaces of the ICM, respectively. These basic structural units form distinct supramolecular arrays in which radiant energy harvested by B800–850 is transferred to B875, which directs these excitations to the reaction center BChl special pair where they are transduced into a transmembrane charge separation [4].

Recently, the X-ray structure of the homologous LH2 complex from *Rhodopseudomonas acidophila* was elucidated at 2.5 Å resolution [5] and shown to form a ring-like assembly, with transmembrane α-helices of nine β- and nine α-apoproteins making up the respective outer and inner walls (outer and inner diameters of 68 and 36 Å, respectively). A continuous overlapping ring of 18 B850 BChl molecules is sandwiched between them, while the nine B800 BChls are positioned on the outside surface and the carotenoids are intertwined with the phytol chains of the BChls, spanning most of the membrane. A similar structure consisting of eight α- and β-units has subsequently been determined for the crystalline LH2 complex of *Rhodospirillum molischianum* [6]. A cryo-electron microscopy analysis of two-dimensional crystals formed from the *Rhodospirillum rubrum* LH1 complex at a resolution of 8.5 Å has revealed a ring-like structure with a 116 Å outside diameter [7], in which densities were assigned to 16 αβ-heterodimers containing an overlapping ring of 32 BChls. Although membrane-embedded domains of a single reaction center fit within the interior of the LH1 ring, recent pigment analyses on various species of purple bacteria indicated a lower LH1-BChl to reaction center ratio of 25±3 [8].

At the level of supramolecular organization, Monger and Parson [9] concluded on the basis of singlet-triplet quenching efficiencies in various strains of *R. sphaeroides* that clusters of B875 complexes surround and interconnect reaction centers, with B800–850 complexes arranged peripherally in large 'lakes'. Subsequent singlet-singlet annihilation measurements provided a detailed refinement of this proposal, as well as estimates of the size and organization of antenna domains in ICM vesicles (chromatophores) from a variety of photosynthetic bacteria [10–16]. Results for *R. sphaeroides* [11] were explained by an arrangement in which three to four reaction centers are embedded in core assemblies of ∼100 B875 BChl molecules, with B800–850 units of ∼45 B850 BChls interspersed between them. Whereas at room temperature, many reaction centers are interconnected as a result of energy equilibration over B850 and B875 BChls [17], at 4 K, such core clusters become thermally separated. Ultrafast polarized light spectroscopy has permitted resolution of energy transfer events that occur at all temperatures within about 400 fs, ascribed to rapid diffusion among the BChls within a single pigment-protein complex [18–21]. Equilibration over spectrally inhomogeneous antenna sites on 1–10 ps time scale was inferred from fluorescence decay kinetics [22], while the transfer of excitations from LH2 to LH1, with time constants of 3 and 5 ps at 300 K and 77 K, respectively, was shown [23] to proceed by the Förster mechanism. More recently, femtosecond pump-probe measurements at room temperature [24] in membranes from an *R. sphaeroides* strain lacking reaction centers have demonstrated multiphasic energy transfer from B850 to B875 BChl with time constants of ∼4.5 and 25 ps. The fast step was attributed to direct transfer from LH2 in contact with LH1 and the slower one to migration of excitations among B850 BChl rings remote from LH1, preceding eventual transfer to the core antenna. In addition, it was shown that excitation energy does not fully equilibrate over LH2 and LH1 within 200 ps in these membranes.

In the present study, functional associations between pigment-protein complexes within the membrane are investigated by spectroscopic studies on *R. sphaeroides* chromatophores fused with unilamellar liposomes. Such bilayer dilution procedures have been applied in the past to assess diffusional and collisional interactions that mediate electron transfer in both mitochondrial membranes [25] and chroma-

tophores [26–28]. Although the previously used low-pH mediated and Ca^{2+}-induced fusion techniques resulted in losses of B800 BChl from *R. sphaeroides* chromatophores [29], a lipid-induced dissociation of B800–850 from photosynthetic core units was suggested from a reduction in the efficiency of energy transfer from B850 to B875. In contrast, it has been reported that when *R. capsulatus* chromatophores were fused to liposomes, enhanced fluorescence arose exclusively from LH1 [30].

Here, a modified freeze-thaw-sonication technique is presented that facilitated preparation of membranes with controlled levels of lipid enrichment and improved yields, in which pigment-protein interactions remained intact. Based upon singlet-singlet annihilation and other fluorescence yield measurements on a series of preparations with gradual lipid-to-protein ratio increases of up to 15-fold, core assemblies, containing about 50 B875 BChls, are thought to be fragmented into units of about half their original size as a result of bilayer dilution. The estimated size of physically detached intact B800–850 clusters is in approximate agreement with that of single rings, suggesting that efficient energy transfer in the membrane relies on dense packing of the complexes, rather than on specific inter-molecular interactions.

2. Materials and methods

Procedures for photoheterotrophic growth [31] of *R. sphaeroides* NCIB 8253 and chromatophore preparation [32] have been described previously. For preparation of liposomes, crude soybean phosphatidylcholine (100 mg) (Sigma, St. Louis, MO), purified

as described by Westerhuis [33], was suspended in 1 ml of 50 mM HEPES/50 mM KCl buffer (pH 7.5) in a pyrex tube, clarified by sonication under nitrogen at $20 \pm 4°C$ in a bath sonicator (Heat Systems-Ultrasonics, Plainview, NY), and centrifuged at 10 000 rpm for 10 min to remove remaining multilamellar vesicles. A modification of the procedure of Casadio et al. [34] was used to prepare phospholipid-enriched membranes in which varying amounts of liposomes were added to 0.5 ml of chromatophores (1 mM BChl in 50 mM HEPES/10 mM $MgCl_2$ buffer, pH 7.5) and the volume was adjusted to 1.0 ml with HEPES-KCl buffer. These chromatophore-liposome mixtures were subjected to five cycles of freeze-thaw sonication, with thawing at 5°C and a 1-min sonication (2 min during last cycle) at 25°C. Preparations were layered onto 0–40% (w/w) sucrose density gradients prepared in 50 mM HEPES/5 mM $MgCl_2$ (pH 7.5) and centrifuged for 18 h at $130 000 \times g$. Pigmented bands were washed at $360 000 \times g$ for 60 min and resuspended in 1 mM Tris-HCl buffer, pH 7.5. Membrane preparations were assayed for BChl, protein and phospholipid contents as described previously [29] and stored in 25% (v/v) glycerol at −80°C.

For freeze-fracture electron microscopy [35], membrane preparations were rapidly plunged into liquid propane and fractured in a Balzers model 301 freeze-etch apparatus at a stage temperature of −170°C and a vacuum of at least 1×10^{-7} Torr. Specimens were shadowed with platinum at 45°, replicas were backed with carbon (90°), rinsed in distilled water and viewed in a JEOL JEM-100 CXII electron microscope at 80 kV.

Low-temperature absorption, fluorescence emission and excitation spectra were obtained on an ap-

Table 1
Composition and sedimentation properties of chromatophore-liposome fusion products

Preparation	Mixing ratio[a]	Buoyant density	BChl/protein	Phospholipid/protein	
		(g/ml)	(μg/mg)	(mg/mg)	-fold increase
1	0:1	1.156	62.5	0.30	1.0
2	2:1	1.137	67.0	0.65	2.2
3	5:1	1.112	63.0	1.1	3.7
4	10:1	1.077	64.5	1.9	6.3
5	15:1	1.059	61.0	4.0	13
6	20:1	1.055	61.5	4.4	15

[a]Liposome/chromatophore phospholipid (w/w).

paratus described previously [36]. For singlet-singlet annihilation measurements, excitations were generated with 532-nm pulses from a frequency doubled Nd:YAG laser with a maximum pulse energy of ~ 5 mJ/cm and a width of ~ 35 ps, using the apparatus in [11]. Reaction centers were maintained in a photo-oxidized state with continuous background illumination.

Fluorescence polarization measurements were performed as described by Westerhuis et al. [37], using a Johnson Research Foundation DBS-3 spectrophotometer, modified for fluorescence spectroscopy and to accommodate an Oxford DN1704 liquid nitrogen cryostat, and HR sheet polarizers (Polaroid Corporation, Cambridge, MA). A 935-nm band-pass filter of 10-nm half-band width (Omega Optical, Brattleboro, VT) was used for detection. Polarization values are given by: $p = (I_{\parallel} - I_{\perp})/(I_{\parallel} + I_{\perp})$, where $I_{\parallel}$ and $I_{\perp}$ are the relative fluorescence intensities with polarization either parallel or perpendicular, respectively, to the polarization direction of the excitation light. Corrections were made for residual transmission resulting from incomplete blockage of the perpendicular component of the electric vector as described by Westerhuis and Niederman (in preparation).

3. Results

3.1. Characterization of fusion products

The yield of the chromatophore-liposome fusion procedure of Casadio et al. [34] was improved by repeating the freeze-thaw-sonication cycles up to
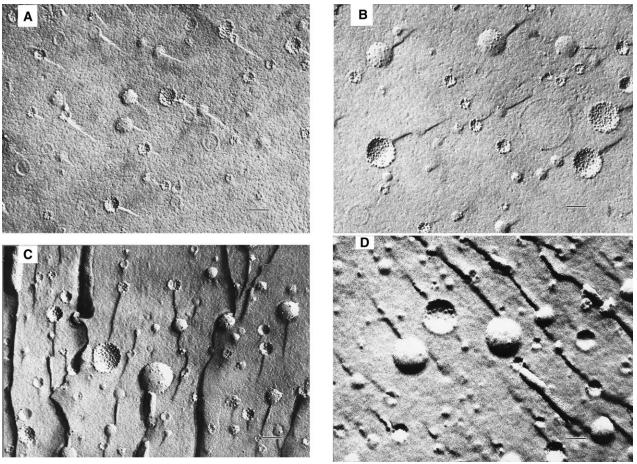

Fig. 1. Electron micrographs of freeze-fracture replicas of phospholipid-enriched chromatophore preparations. (A) Control chromatophores. (B–D) Liposome-chromatophore fusion products with increases in phospholipid/protein (w/w) ratios of 3.5-, 5.0- and 8.0-fold, respectively. Shadowing was from left to right. A 100-nm scale bar is shown in each panel.
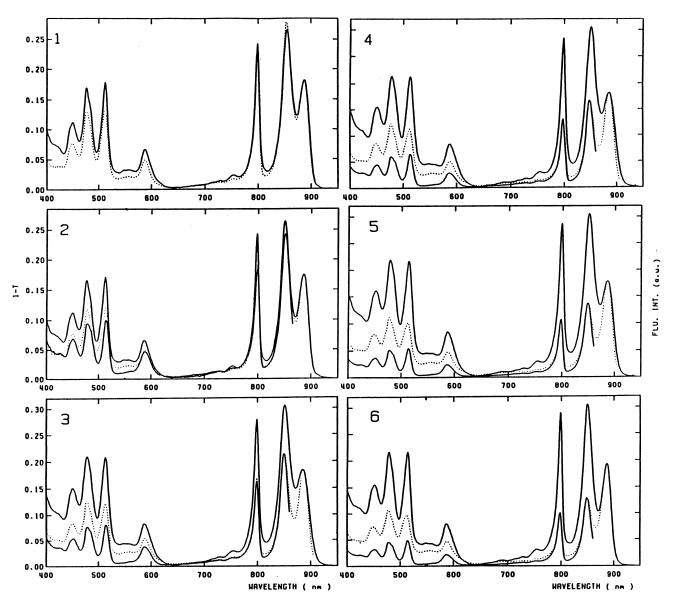
Fig. 2. Absorption and fluorescence excitation spectra of phospholipid-enriched chromatophore preparations at 4 K. Preparations 1–6 used for these measurements and those described in Figs. 3 and 4 are from Table 1. Fractional absorption spectra (upper solid traces) were corrected for scattering by linear baseline subtraction. Excitation spectra of emission from B875 (dotted traces, detection at 915 nm) and from B850 (lower solid traces, detection at 860–870 nm) are normalized at their respective absorption maxima; a.u., arbitrary units.

five times, which resulted in essentially quantitative incorporation of chromatophores, while ∼60–80% of the added lipid appeared in the fusion products. The series of discrete bands present in sucrose density gradients after a single cycle was replaced by a more uniform population of fusion products, with lipid-enrichment proportional to the amount of liposomes initially present. The resulting preparations had incrementally elevated phospholipid contents of up to ∼15-fold (Table 1), while their specific BChl contents and absorption spectra (see below) showed that little or no pigment loss had occurred.

Electron micrographs of freeze-fracture replicas confirmed that bilayer fusion had occurred and showed that the fusion products consisted of closed vesicles of increased size with diminished intramem-
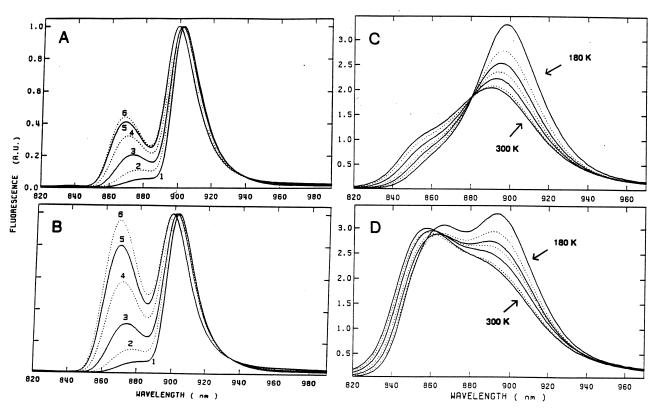
Fig. 3. Fluorescence emission spectra of phospholipid-enriched chromatophore preparations. All spectra were corrected for response of measuring system. (A) Excitation at 590 nm. (B) Excitation at 800 nm; these spectra were measured at 4 K and normalized at emission maxima. (C, D) Temperature dependence of fluorescence emission between 300 and 180 K for control chromatophores (C) and for phospholipid-enriched preparation 5 (D). Alternating solid and dotted traces represent 20 K temperature intervals; these spectra were not normalized. BChl concentration of both samples was the same (± 10%); excitation at 800 nm.

brane particle lateral densities (Fig. 1). Although not closely correlated with lipid enrichment, their diameters were up to 4-fold greater than in unfused chromatophores. Intramembrane particles with approximate diameters of ~100 Å were located mainly on the PF (concave) fracture faces, indicating that chromatophore membrane asymmetry had been largely retained. In more highly enriched preparations, particles were either in small clusters or separated by as much as 500 Å; however, marked intramembrane particle aggregation, as reported by Rivas et al. [38] after low-temperature fusion of chromatophores to phosphatidylserine liposomes, was not observed.

3.2. Absorption and fluorescence measurements

Absorption spectra at 4 K demonstrated that the various absorption bands, especially that of the labile B800 BChl, were retained upon phospholipid enrich-

ment (Fig. 2). Intactness of the peripheral antenna complex was further apparent from the fluorescence excitation spectra of B850 emission, although both the B850 absorption and emission (Fig. 3) maxima were shifted to shorter wavelengths, by up to 5 and 13 nm, respectively (Table 2). The core antenna exhibited a small blue shift mainly in emission spectra.

Fluorescence excitation spectra of core antenna emission (Fig. 2) revealed gradual decreases in energy transfer efficiency between B850 and B875 (ϕ_{et}) from close to 100% to <40% (Table 2). This was also reflected by a significant enhancement of relative fluorescence yield from B850 BChl, up to nearly 20-fold, upon selective excitation of the peripheral antenna at 4 K (Fig. 3A,B). The relative fluorescence yields of the two antenna components depend upon the initial distribution of excitations, the fluorescence lifetimes in the absence of energy transfer and the efficiencies of energy transfer from B850 to B875

(ϕ_{et}) and from B875 to reaction centers (ϕ_{rc}). Therefore, relative fluorescence yields were used to assess the effect of bilayer dilution upon ϕ_{rc}, assuming that the intrinsic decay rates for B850 and B875 BChls were the same. Estimates of the loss yields in LH1 ($\phi_l^c = 1 - \phi_{rc}$) based upon the relative fluorescence yields [33] are shown in Table 2. For preparation 1, this did not give a meaningful result because the B850 to B875 transfer efficiency was unity within experimental error, but assuming $\phi_{et} = 0.98$ yielded a loss yield (~ 0.25) in agreement with the notion that in native chromatophores, photooxidized reaction centers still quench $\sim 70\%$ of core antenna fluorescence at 4 K [11,40]. For each of the more highly enriched preparations (3–6), the loss yield in LH1 was estimated to be close to 1.00. Despite the uncertainty in these estimates (± 0.25), they too suggested that lipid enrichment had resulted in a reduction in energy transfer from B875 to reaction centers from about 70% [11] to less than 25%.

The temperature dependence of the equilibration of excitation energy over the two antenna components was examined by emission spectra in the range of 180–300 K, at 20 K intervals, for the control and a highly lipid-enriched preparation. In this temperature range, lipid enrichment resulted in a 3.5–4.5-fold increase in the B850 fluorescence yield, upon excitation at either 590 or 800 nm. However, the absolute fluorescence yield from the core antenna was diminished by less than 20% when excitation was at 800 nm (Fig. 3C,D), and increased nearly 2-fold as a result of bilayer dilution when the core antenna was excited more directly at 590 nm (not shown). A similar fusion-induced increase in absolute fluorescence yield from the core was found upon excitation at 532 nm with weak laser flashes (see below). These observations showed that altered relative fluorescence yields were due to enhanced core antenna fluorescence, rather than to increased non-radiative decay in the peripheral antenna, and confirmed that bilayer dilution had also resulted in reduced connectivity of LH1 and reaction centers.

3.3. Singlet-singlet annihilation measurements

While steady-state fluorescence spectroscopy demonstrated a lipid-induced reduction in energy transfer between the various complexes, the extent of energy transfer within both the peripheral antenna and the core structures was further examined by estimating functional domain sizes (N_D) from singlet-singlet annihilation measurements. Annihilation curves, with

Table 2
Absorption and emission maxima and energy transfer properties of phospholipid-enriched chromatophore preparations at 4 K

	Absorption		Emission		ϕ_{et}^a	ΦB850/ΦB875[b]		$(\phi_l^c)^c$	
	maxima	(nm)	maxima	(nm)		excitation	(nm)	excitation	(nm)
preparation	B850	B875	B850	B875		590	800	590	800
1	854	887	881	902	1.02	0.05	0.07	–	–
2	850	885	877	902	0.91	0.14	0.20	0.41	0.45
3	851	885	873	901	0.67	0.25	0.38	1.06	1.14
4	851	886	871	900	0.50	0.40	0.70	1.14	1.21
5	850	886	869	899	0.40	0.53	1.03	1.11	1.15
6	849	886	868	899	0.37	0.57	1.23	1.13	1.11

[a] ϕ_{et}, efficiency of B850→B875 energy transfer (± 0.05) determined from ratio of peak heights near 850 nm in excitation and fractional absorption spectra, after normalization at B875 band (Fig. 2).
[b] ΦB850/ΦB875, relative fluorescence yields (± 0.05) determined from relative heights of 4 K emission maxima (Fig. 3). Corrected for spectral overlap of both components at the B875 emission maxima by subtracting the 4 K emission spectrum of mutant strain NF57 [39], which contains B800–850 as the sole antenna complex, after alignment and normalization of the spectra at the respective B850 bands. Spectral overlap near the B850 emission maximum is negligible at 4 K [39]. Fluorescence bandwidth differences were accounted for by multiplying the ratio of B850 and B875 emission maxima by a factor 1.15.
[c] The expression is the loss yield in the core antenna (fraction of excitations lost via radiative or non-radiative decay with phototraps closed [11], ± 0.25), calculated using an expression for energy equilibration over a two-component antenna under steady-state conditions [33]. At 4 K, $1/\phi_l^c = \Phi$B850/ΦB875 $(1/(\alpha(1-\phi_{et}))-1)$, with α the fraction of excitations located initially in the peripheral antenna (0.62 and 0.91 at 590 and 800 nm, respectively), assuming equal rates for radiative and non-radiative decay in both antenna components.

time-integrated fluorescence yield plotted as a function of incident energy density of exciting laser flashes, are shown in Fig. 4. The experimental data were fitted with quenching curves, generated on the basis of a model that assumes a homogeneous lattice of interconnected pigments over which excitation energy migrates randomly [41,42]. The shape of these curves depends upon the probability of annihilation, defined as:

$$r = \frac{2\gamma_1}{\gamma_2} \tag{1}$$

where γ_1 is the effective rate constant for all monomolecular decay processes combined, and γ_2 is the effective rate constant for annihilation (i.e., an effective first order rate constant) which depends upon the 'hopping rate' of an excitation as well as on domain size.

Annihilation curves for B875 emission at 4 K, each of which was fitted with $r = 1$ (Fig. 4A), exhibited a shift to higher energy densities as lipid enrichment increased, indicating a diminution in core domain sizes. Domain size estimates were calculated as described elsewhere [11], using the B875 BChl concentration, the density of the incident photon flux, the fractional absorption at 532 nm, and the efficiency of energy transfer from carotenoids to B875 BChl, either directly or through the B800–850 complex. Annihilation within the peripheral antenna, prior to transfer to the cores, was neglected since incident energies required to generate a single excitation per B875 domain were insufficient to cause significant quenching of B850 fluorescence (Fig. 4B). The quenching curves and the calculated domain sizes (Table 3, N_D values not in brackets) for control chromatophores were essentially the same as those reported previously by Vos et al. [11]. Bilayer dilution resulted in a reduction in cluster size for preparations 2 and 3 by about 30%, while further lipid enrichment (preparation 5) appeared to reduce the cores to nearly half their original size.

The 4 K annihilation curves of B850 emission for preparations 3 and 5, which nearly coincided, were fitted with r values of 2 and 1, respectively (Fig. 4B). The respective domain sizes were calculated based on the B850 BChl concentrations and the fraction of excitations located initially in the peripheral antenna (40%). The difference in resulting estimates of ~ 55
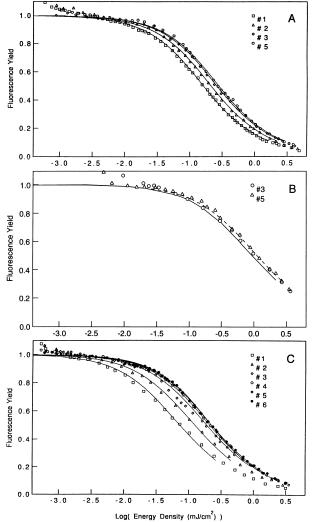

Fig. 4. Singlet-singlet annihilation curves for quenching of fluorescence in phospholipid-enriched chromatophore preparations. The time-integrated fluorescence yield is plotted as a function of incident energy using excitation at 532 nm as described in the text; numbers in the upper right-hand corner of each panel identify preparations. (A) Fluorescence from B875 at 4 K, detection at 915 nm. (B) Fluorescence from B850 at 4 K, detection at 880 nm. (C) Fluorescence from B875 at 300 K, detection at 910 nm. Domain sizes calculated from these data are presented in Table 3.

and 110 reflects the uncertainty in the fits (i.e., the r value choices), rather than an actual difference in connectivity, which was comparable to that obtained for wild-type chromatophores ($N_D = 45$, $r = 1$) [11], but somewhat greater than for the LH2-only mutant NF57 ($N_D = 30$, $r = 1$) [43].

Annihilation curves of B875 fluorescence at 300 K

Table 3
Antenna domain size estimates for phospholipid-enriched chromatophore preparations[a]

Preparation	4 K						300 K		
	B875 emission			B850 emission			B875 emission		
	r	N_D		r	N_D		r	N_D	
1	1	89	[41][b]	–	–[c]	–	> 5	> 350	[48]
2	1	64	[29]	–	–	–	> 5	> 230	[32]
3	1	63	[29]	2	109	[30]	3	145	[34]
4	–	–	–	–	–	–	2	93	[26]
5	1	51	[24]	1	57	[25]	2	104	[29]
6	–	–	–	–	–	–	1	71	[34]

[a]Preparations used for these measurements are from Table 1.

[b]Values in brackets denote domain size estimates corresponding to $r = 0$, calculated from the energy densities where the fluorescence yield had decreased to $1 - 1/e$ of the value for low energy excitation as further explained in the text.

[c]The size of LH2 domains at 4 K could not be estimated in control chromatophores, since as a result of efficient downhill energy transfer, nearly all fluorescence arose from the core antenna, even upon direct excitation of the peripheral complex at 800 nm.

(Fig. 4C) revealed a considerable shift toward higher incident energies for membranes with only 4-fold lipid enrichment. Despite an additional 4-fold increase in lipid content, the curves for the most highly enriched membranes were shifted only marginally further. The excitation densities in LH1 at 300 K were estimated by assuming rapid equilibration between LH1 and a fraction of LH2, given by the transfer efficiencies at 4 K, with the remaining LH2 fully dissociated. The B875 domain size at 300 K ($N_D > 350$, $r > 5$, Table 3) obtained for the control
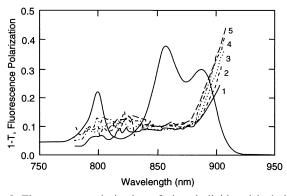
is somewhat smaller than that reported earlier [11] ($N_D = 1000$, $r = 2$), but similar to that found in [15] ($N_D > 397$) for the same r value. The more highly lipid-enriched membranes, fitted with $r = 1-2$, yielded core domain size estimates of $\sim 70-100$ (Table 3), again reflecting differences in the fitting parameter r. The significance of these estimates and those based on fits with $r = 0$ (Table 3) is discussed further below.

3.4. Fluorescence polarization measurements

Fluorescence polarization spectra at 77 K of the various membrane preparations were obtained as an alternative means for examining aggregation states of

Fig. 5. Fluorescence polarization of phospholipid-enriched chromatophore preparations at 77 K. The 77 K fractional absorption $(1 - T)$ spectrum of the control chromatophores (preparation 1) is included to show the relation of the fluorescence polarization (p) to the various regions of the near-IR absorption bands. Preparations 2, 3, 4 and 5 were lipid enriched by 3.5-, 5.0-, 7.3- and 11.4-fold, respectively; their B875 absorption maxima were blue-shifted by 1–4 nm with increasing enrichment level.

Table 4
Relative overlap integrals for energy transfer among antenna complexes

	LH2→LH1	LH1→LH2	LH2→LH2	LH1→LH1
300 K	1.00[a]	0.31	1.21	1.06
4 K (native)	0.53	0.00	0.03	0.28
4 K (fused)	0.18	0.00	0.13	0.34

[a]Overlap integrals, relative to the overlap for LH2→LH1 transfer at 300 K, were calculated by approximating absorption and emission spectra of chromatophores by Gaussians with widths (FWHM) of about 40 nm at 300 K and 18 nm at 4 K, and respective center wavelengths at 850 and 857 nm (LH2, 300 K), 875 and 893 nm (LH1, 300 K), 854 and 881 nm (LH2, 4 K), and 887 and 902 nm (LH1, 4 K), based on spectra obtained here and in [39]. For chromatophore-liposome fusion products, 4 K absorption and emission maxima were taken as 849 and 868 nm (LH2), and 886 and 899 nm (LH1).
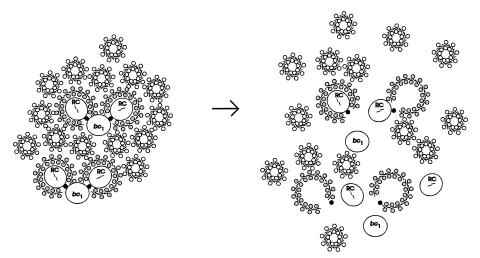
Fig. 6. Model for the organization of the light harvesting antenna in *R. sphaeroides* in plane of membrane, and the effects of bilayer dilution. Arrays of small stippled circles represent the LH1 transmembrane helices showing B875 BChls sandwiched between them; smaller arrays of open circles represent LH2 rings with B850 BChl sandwiched in between. A possible association of reaction centers (RC, with BChl dimers shown in center) and cytochrome bc_1 complex (bc_1) via the PufX protein, required for proper organization of the LH1 complex [37] (single solid circles), is also shown. On the right, LH2 dissociation, fragmentation of the LH1 ring structure and a reduction of LH1-reaction center connectivity are depicted.

the core complex (Fig. 5). Bilayer dilution resulted in a gradual increase in the magnitude of the anisotropic long-wavelength component of the B875 Q_y absorption band. While attributed originally to a distinct long-wavelength subantenna ('B896') [44], this is now believed to be largely a manifestation of site inhomogeneity [22,45]. The enhanced polarization values are in agreement with reduced connectivity of inhomogeneous pigment clusters [45], and have been observed experimentally with LH1 oligomers of reduced aggregation state isolated by LDS-polyacrylamide gel electrophoresis (Westerhuis and Niederman, in preparation).

4. Discussion

4.1. Effects of bilayer dilution upon energy transfer

The repeated cycles of freeze-thaw-sonication used in this study to improve the efficiency of chromatophore-liposome fusion, resulted in quantitative lipid incorporation and preparations suitable for examining the effects of gradual bilayer dilution on antenna connectivity. Although low-temperature absorption spectra indicated that the light-harvesting complexes, including the labile B800 BChl component, remained

intact during fusion, blue shifts of up to 5 nm were seen in the absorption of the B850 band. These were also observed when LDS is replaced with LDAO in the isolated LH2 complex [46], and may arise from minor conformational changes in detergent micelle or expanded bilayer environments.

Further analysis of the altered energy transfer and fluorescence yield properties observed for the lipid-enriched preparations requires consideration of both antenna structure and energy transfer dynamics. The rate of energy transfer by inductive resonance is given by the Förster equation:

$$k_{et} = \frac{1}{\tau_o}\left(\frac{R_o}{R}\right)^6 \tag{2}$$

where τ_o is the fluorescence lifetime in the absence of energy transfer, R is the inter-chromophore center-to-center distance, and R_o is determined by the dipole orientations and temperature-dependent spectral overlap of the donor-acceptor pair. Both B850 and B875 BChls are organized into ring-like structures in which ultrafast (<1 ps) energy transfer occurs [20,47], while excitation migration and energy trapping by the reaction center are dependent on transfer among clusters of LH2 and core complexes. Models for their arrangement [24,47] propose that some LH2 forms remote pools which would contrib-

ute to the multiphasic LH2→LH1 energy transfer kinetics between 300 and 77 K [24,48]. The fast time constant (3–5 ps), attributed to transfer at LH2-LH1 contact sites, suggests a minimum distance between chromophores on adjacent rings of ∼30 Å [23], while the slow component (∼25 ps) reflects transfer among remote LH2 rings prior to transfer to the cores [24]. However, the high efficiency of LH2→LH1 transfer in the intact chromatophore preparations (Table 2) shows that at 4 K, excitation transfer at LH2-LH1 contact sites must still be quite rapid (<15 ps), based on a fluorescence lifetime of 350 ps [49].

Assuming similar B850 and B875 BChl organization and chromophore geometries at contact sites, energy transfer efficiencies between two adjacent complexes will largely depend upon respective spectral overlap integrals, estimated here from overall spectral features (Table 4). Although inhomogeneity of site energies, which becomes important at low temperatures [50], was not taken into account, these data agree with the >10-fold reduction in transfer rate (100–150 ps) among LH2 complexes upon cooling to 4 K [43]. They are also supported by the weak temperature dependence of LH2→LH1 transfer, explained by the large LH2 Stokes shift at 4 K, and a large, nearly temperature-independent spectral overlap between LH2 emission and LH1 absorption. Thus, the slowed k_{et} among LH2 complexes at 4 K, together with the τ_o of 350 ps, imply that transfer of peripheral LH2 to LH1 occurs with >25% loss. Since the overall loss was <5%, >80% of the LH2 complexes must transfer directly to adjacent LH1, in agreement with amplitude ratios of the fast and slow components of B850 fluorescence decay at 77 K [48].

The gradual reductions in the efficiency of LH2→LH1 transfer induced by bilayer dilution could be explained by either uniform decreases in k_{et} at all LH2-LH1 contact sites, or by an increasing fraction of LH2 complexes becoming fully dissociated. Assuming that excess lipid is interspersed evenly between LH2 and core complexes, a <40% transfer efficiency at 4 K and a τ_o of 350 ps would imply an effective transfer time of 500 ps. Compared to intact chromatophores this would suggest a reduction in the k_{et} of between 35- and 100-fold. Since the blue-shifted LH2 emission would account for a ∼3-

fold decrease in average overlap integral, the remaining 10–35-fold reduction could be ascribed to a uniform increase in inter-complex BChl-BChl distance from about 30 Å in densely packed chromatophores [23], to 45–55 Å in highly diluted membranes, corresponding to ring separations of 15–25 Å. However, a less uniform dissociation seems more likely from the freeze-fracture replicas.

4.2. Excitation annihilation in native and lipid-enriched membranes

The rapid decrease in LH1 domain sizes at 300 K after moderate lipid enrichment, as opposed to more gradual losses in LH2→LH1 transfer, can be explained by the requirement of at least two close LH1-LH2 contact sites for transfer between two LH1 clusters via LH2, that will thus exhibit a greater sensitivity to LH2 dissociation. Due to rapid migration within a single ring (<1 ps [20]), the diffusion rate will be determined mainly by transfer between LH1 complexes, with a time constant of <5 ps, similar to that for LH2→LH1 transfer. Thus, annihilation in these domains should be extremely efficient ($1/\gamma_2 < 20$ ps), with quenching curves exhibiting r values of <0.2 (Eq. 1, $1/\gamma_1 = 200$ ps). The shallower curves (with apparent r values of 1) may reflect non-uniformities, either in actual cluster sizes or from spatial inhomogeneity in the exciting laser beam. In either case, the number of excitations created per domain would vary, leading to superposition of steeper ($r = 0$) curves distributed around an average. Thus, estimates of the average domain size using $r = 0$ appear more plausible (Table 3, bracketed values).

Since at low temperatures spectral inhomogeneity would lead to rapid localization of excitations at low-energy sites [50], the same argument applies to the 4 K annihilation curves. For each fused preparation, this results again in domain sizes corresponding to single B875 complexes (Table 3), whereas in native membranes, excitations would diffuse over nearly two full rings. The resulting estimates for LH2 (25–30 B850 BChls) also correspond to an average cluster size of one to two rings [5,6].

The LH2:LH1 stoichiometry in native chromatophores (∼1.75) and the relative sizes of the complexes suggest that a regular hexagonal arrangement

is possible with monomeric core complexes entirely surrounded by LH2. Such well-ordered arrangements have been suggested recently [47] on the basis of structural information [5,7], together with molecular modeling [51]. Nevertheless, our results suggest the possibility that a significant fraction of LH1 complexes occur in clusters of two. While this may represent an average value due to random distribution of LH1 rings, it could also reflect functional associations of LH1-reaction center core complexes. The latter proposal, considered in the model shown in Fig. 6, is supported by the rectangular particles seen in freeze-fracture replicas of tubular membranes in M21 (LH2⁻) cells, interpreted to contain a pair of reaction centers surrounded by LH1 arrays (Westerhuis and Niederman, in preparation). Sabaty et al. [52] have noted that these could represent supercomplexes that include a cytochrome bc_1 complex [53]. Fig. 6 also considers the possibility that the PufX protein is interspersed into the LH1 ring, interrupting formation of complete circles, and providing a possible basis for LH1-reaction center dissociation.

Finally, the interpretation of 4 K annihilation curves resolves a paradox concerning the relationship of fluorescence polarization spectra to LH1 domain sizes. Rises in fluorescence polarization over the red wing of the B875 absorption band were initially explained by emission from an anisotropic low-energy component ('B896') [44], accounting for $\sim 15\%$ of the overall Q_y band; with LH1 domains of 75–100 BChls [11,12], this would correspond to a subpool of 12–15 pigments. Such low-energy sites restrict the diffusion length of excitations, causing annihilation to occur primarily in long-wavelength pigment clusters. N_D would then be determined by antenna size per low-energy cluster and each domain would contain only a single subpool of interconnected low-energy sites. The original N_D estimates therefore implied that the anisotropic component consists of highly organized clusters containing more than ten nearly parallel dipole moments, which is difficult to reconcile with antenna ring structures. However, with LH1 domains of 40–50 BChls, the dipole strength of the low energy component would be equivalent to that of only 6–8 BChls. The circular antenna pigment organization suggests that this component corresponds to a single excitonic state of 6–8 coupled chromophores, rather than a subpool of par-

allel transition dipoles. This agrees reasonably well with dipole strength determined for emitting components [54,55] relative to that of monomeric BChl for LH1 and LH2, as well as for the $(\alpha\beta)BChl_2$ B820 subunit [56], at both 300 and 4 K.

References

[1] R. Theiler, F. Suter, H. Zuber, R.J. Cogdell, FEBS Lett. 175 (1984) 231–237.

[2] R. Theiler, F. Suter, J.D. Pennoyer, H. Zuber, R.A. Niederman, FEBS Lett. 184 (1985) 231–236.

[3] H. Zuber, in: G. Drews, E.A. Dawes (Eds.), Molecular Biology of Membrane-Bound Complexes in Phototrophic Bacteria, Plenum, New York, 1990, pp. 161–180.

[4] R. van Grondelle, J.P. Dekker, T. Gillbro, V. Sundström, Biochim. Biophys. Acta 1187 (1994) 1–65.

[5] G. McDermott, S.M. Prince, A.A. Freer, A.M. Hawthornthwaite-Lawless, M.Z. Papiz, R.J. Cogdell, N.W. Isaacs, Nature 374 (1995) 517–521.

[6] J. Koepke, X. Hu, C. Muenke, K. Schulten, H. Michel, Structure 4 (1996) 581–597.

[7] S. Karrasch, P.A. Bullough, R. Ghosh, EMBO J. 14 (1995) 631–638.

[8] C. Francke, J. Amesz, Photosynth. Res. 46 (1995) 347–352.

[9] T.G. Monger, W.W. Parson, Biochim. Biophys. Acta 460 (1977) 393–407.

[10] J.G.C. Bakker, R. van Grondelle, W.T.F. Den Hollander, Biochim. Biophys. Acta 725 (1983) 508–518.

[11] M. Vos, R. van Grondelle, F.W. van der Kooij, D. van de Poll, J. Amesz, L.N.M. Duysens, Biochim. Biophys. Acta 850 (1986) 501–512.

[12] G. Deinum, T.J. Aartsma, R. van Grondelle, J. Amesz, Biochim. Biophys. Acta 976 (1989) 63–69.

[13] G. Deinum, S.C.M. Otte, A.T. Gardiner, T.J. Aartsma, R.J. Cogdell, J. Amesz, Biochim. Biophys. Acta 1060 (1991) 125–131.

[14] H. Kramer, G. Deinum, A.T. Gardiner, R.J. Cogdell, C. Francke, T.J. Aartsma, J. Amesz, Biochim. Biophys. Acta 1231 (1995) 33–40.

[15] H. Kramer, M.R. Jones, G.J.S. Fowler, C. Francke, T.J. Aartsma, C.N. Hunter, J. Amesz, Biochim. Biophys. Acta 1231 (1995) 89–97.

[16] H. Kramer, J. Amesz, Photosynth. Res. 49 (1996) 237–244.

[17] K.L. Zankel, R.K. Clayton, Photochem. Photobiol. 9 (1968) 7–15.

[18] H.M. Visser, O.J.G. Somsen, F. Van Mourik, R. Van Grondelle, J. Phys. Chem. B 100 (1996) 18859–18867.

[19] T. Pullerits, M. Chachisvilis, M.R. Jones, C.N. Hunter, V. Sundström, Chem. Phys. Lett. 24 (1994) 355–365.

[20] S.E. Bradforth, R. Jimenez, F. Van Mourik, R. Van Grondelle, G.R. Fleming, J. Phys. Chem. B 99 (1995) 16179–16191.

[21] J.T.M. Kennis, A.M. Streltsov, T.J. Aartsma, T. Nozawa, J. Amesz, J. Phys. Chem. B 100 (1996) 2438–2442.

[22] K. Timpmann, A. Freiberg, V.I. Godik, Chem. Phys. Lett. 182 (1991) 617–622.

[23] S. Hess, M. Chachisvilis, K. Timpmann, M.R. Jones, G.J.S. Fowler, C.N. Hunter, V. Sundström, Proc. Natl. Acad. Sci. USA 92 (1995) 12333–12337.

[24] V. Nagarajan, W.W. Parson, Biochemistry 36 (1997) 2300–2306.

[25] H. Schneider, J.J. Lemaster, M. Höchli, C.R. Hackenbrock, J. Biol. Chem. 255 (1980) 3748–3756.

[26] R. Casadio, G. Venturoli, B.A. Melandri, Eur. Biophys. J. 16 (1988) 243–253.

[27] M. Snozzi, A.R. Crofts, Biochim. Biophys. Acta 766 (1984) 451–463.

[28] G. Venturoli, J.G. Fernandez-Velasco, A.R. Crofts, B.A. Melandri, Biochim. Biophys. Acta 851 (1986) 340–352.

[29] J.D. Pennoyer, H.J.M. Kramer, R. van Grondelle, W.H.J. Westerhuis, J. Amesz, R.A. Niederman, FEBS Lett. 182 (1985) 145–150.

[30] J. Takemoto, T. Schonhardt, J.R. Golecki, G. Drews, J. Bacteriol. 162 (1985) 1126–1134.

[31] L.M. Olivera, R.A. Niederman, Biochemistry 32 (1993) 858–866.

[32] C.N. Hunter, J.D. Pennoyer, J.N. Sturgis, D. Farrelly, R.A. Niederman, Biochemistry 27 (1988) 3459–3467.

[33] W.H.J. Westerhuis, Ph.D. Thesis, Rutgers University, New Brunswick, NJ, 1995.

[34] R. Casadio, G. Venturoli, A. DiGioia, P. Castellani, L. Leonardi, B.A. Melandri, J. Biol. Chem. 259 (1984) 9149–9157.

[35] R. Theiler, R.A. Niederman, J. Biol. Chem. 266 (1991) 23157–23162.

[36] R. van Grondelle, H.J.M. Kramer, C.P. Rijgersberg, Biochim. Biophys. Acta 682 (1982) 208–215.

[37] W.H.J. Westerhuis, J.W. Farchaus, R.A. Niederman, Photochem. Photobiol. 58 (1993) 460–463.

[38] E. Rivas, B. Costa, T. Gulik-Krzywicki, F. Reiss-Husson, Biochim. Biophys. Acta 904 (1987) 290–300.

[39] R.J. van Dorssen, C.N. Hunter, R. van Grondelle, A.H. Korenhof, J. Amesz, Biochim. Biophys. Acta 932 (1988) 179–188.

[40] R. van Grondelle, Biochim. Biophys. Acta 811 (1985) 147–195.

[41] G. Paillotin, C.E. Swenberg, J. Breton, N.E. Geacintov, Biophys. J. 25 (1979) 512–533.

[42] W.T.F. Den Hollander, J.G.C. Bakker, R. van Grondelle, Biochim. Biophys. Acta 725 (1983) 492–507.

[43] M. Vos, R.J. van Dorssen, J. Amesz, R. van Grondelle, C.N. Hunter, Biochim. Biophys. Acta 933 (1988) 132–140.

[44] H.J.M. Kramer, J.D. Pennoyer, R. van Grondelle, W.H.J. Westerhuis, R.A. Niederman, J. Amesz, Biochim. Biophys. Acta 767 (1984) 335–344.

[45] F. van Mourik, R. Visschers, R. van Grondelle, Chem. Phys. Lett. 193 (1992) 1–7.

[46] H.J.M. Kramer, R. van Grondelle, C.N. Hunter, W.H.J. Westerhuis, J. Amesz, Biochim. Biophys. Acta 765 (1984) 156–165.

[47] M.Z. Papiz, S.M. Prince, A.M. Hawthornthwaite-Lawless, G. McDermott, A.A. Freer, N.W. Isaacs, R.J. Cogdell, Trends Plant Sci. 1 (1996) 198–206.

[48] A. Freiberg, V.I. Godik, T. Pullerits, K. Timpmann, Biochim. Biophys. Acta 973 (1989) 93–104.

[49] C.N. Hunter, H. Bergström, R. Van Grondelle, V. Sundström, Biochemistry 29 (1990) 3203–3207.

[50] O.J.G. Somsen, F. van Mourik, R. van Grondelle, L. Valkunas, Biophys. J. 66 (1994) 1580–1596.

[51] X. Hu, A. Damjanovic, T. Ritz, K. Schulten, Proc. Natl. Acad. Sci. USA 95 (1998) 5935–5941.

[52] M. Sabaty, J. Jappé, J. Olive, A. Verméglio, Biochim. Biophys. Acta 1187 (1994) 313–323.

[53] P. Joliot, A. Verméglio, A. Joliot, Biochim. Biophys. Acta 975 (1989) 336–345.

[54] R. Monshouwer, M. Abrahamsson, F. van Mourik, R. van Grondelle, J. Phys. Chem. B 101 (1997) 7241–7248.

[55] J.T.M. Kennis, A.M. Streltsov, H. Permentier, T.J. Aartsma, J. Amesz, J. Phys. Chem. B 101 (1997) 8369–8374.

[56] R.W. Visschers, M.C. Chang, F. van Mourik, P.S. Parkes-Loach, B.A. Heller, P.A. Loach, R. van Grondelle, Biochemistry 30 (1991) 5734–5742.